Supporting Information: Characterisation, Selection and Micro-Assembly of Nanowire Laser Systems

Dimitars Jevtics,[†] John McPhillimy,[†] Benoit Guilhabert,[†] Juan A. Alanis,[‡] Hark Hoe Tan,[¶] Chennupati Jagadish,[¶] Martin D. Dawson,[†] Antonio Hurtado,[†] Patrick Parkinson,[‡] and Michael J. Strain[*,†]

[†]*Institute of Photonics, SUPA Department of Physics, University of Strathclyde, Glasgow, United Kingdom*

[‡]*Department of Physics and Astronomy and Photon Science Institute, The University of Manchester, Manchester, United Kingdom*

[¶]*Department of Electronic Materials Engineering, Research School of Physics and Engineering, The Australian National University, Canberra, Australia*

E-mail: michael.strain@strath.ac.uk

Micro-Fabrication

Preparation of the disk Sample

Host substrates used in the project are commercially available quartz disks, depicted in figure S1(a). Prior to the NW deposition and spin-coating, disks were cleaned following the standard solvent procedure: acetone, methanol, isopropanol, followed by DI water cleaning and hotplate bake at 100 degrees for 10 minutes. Alignment markers, on the substrate, were

produced using a laser lithography technique: an epoxy-based negative photoresist (SU-8) was spin-coated onto a quartz disk substrate with a film thickness of 4 μm. A custom-built maskless laser lithography tool (λ = 370 nm) was used to expose the marker patterns that were then developed using EC solvent, as depicted in figures S1(b-c). Prior to the development those were soft baked at 95° C for 1 min. After the marker patterns were fabricated, a thin layer of photopolymer (NOA-65) was spin-coated onto quartz disk samples. The spin-coated layer was cured using a UV lamp. The specific recipe enabled to produce a coating thickness of 4 μm, this was verified with the profilometer measurements. A schematic of the final disk structure is shown in figure S1(c).

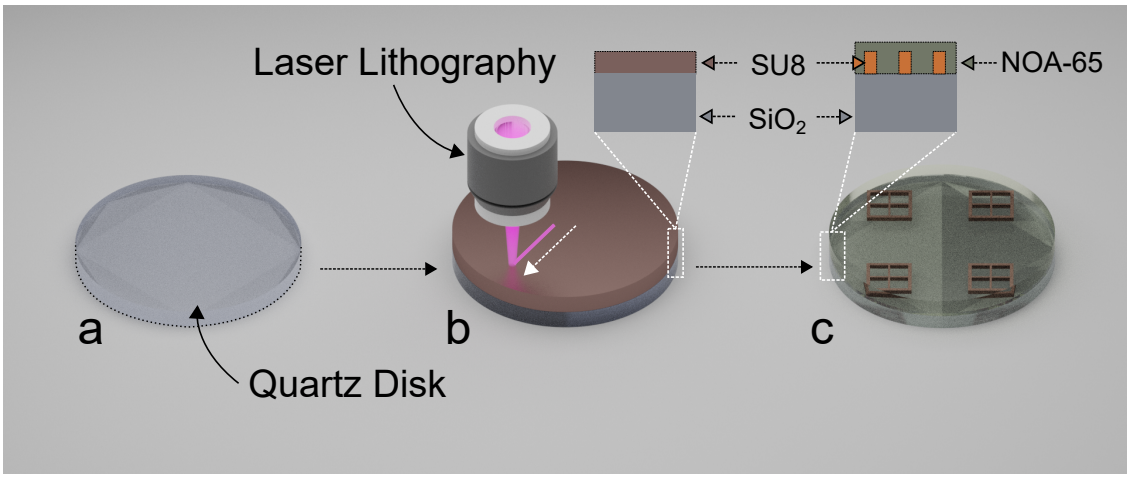

Figure S1: (a) Diagram showing a quartz disk sample. (b) Schematic depiction of the laser lithography process on a quartz disk sample. (c) A quartz disk sample with embedded markers and a polymeric coating layer.

Large-area Integration, Mapping and Printing of NW devices

A slab of PDMS was used to transfer as-grown GaAs-AlGaAs core-shell NW lasers[1] from their growth substrate onto a host quartz disk, as depicted in figures S2(a-d). The PDMS sample was fabricated following the standard recipe and then cut using a scalpel knife forming a square ($\sim$ 2 mm^2) piece. Next, it was mounted as a stamp into the MTP rig and aligned with the GaAs-AlGaAs NW growth sample, as shown in figure S2(a). The NW capture

process was done in two stages shown in figure S2(b): (1) the stamp is controllably pressed onto the NW sample. (2) the stamp is dragged perpendicularly to the NW growth axis for 20 μm which results in breaking NWs' bottom facet and capturing NWs bonded to a tacky stamp's surface.

The stamp with captured NWs was aligned with the target host sample and pressed into the selected area. Following the developed NW capture/release procedure, after raising the stamp from the sample, NW devices with enough surface bonding will be left on the host sample, as graphically shown in figure S2(d). In the last stage we have found that the transfer yield is in the order of 50 %, resulting in a low density distribution of wires.

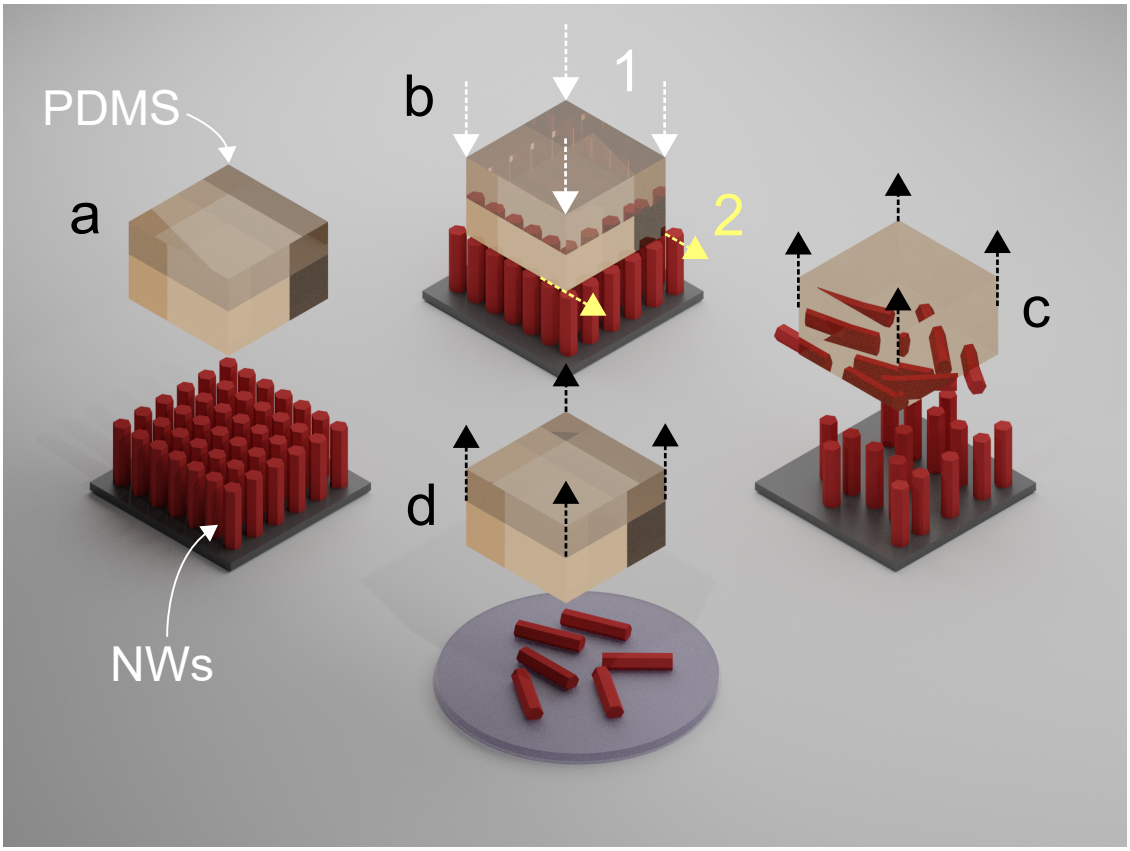

Figure S2: Transfer-printing process of as-grown NW lasers from their growth substrate onto a quartz disk sample: (a) a PDMS slab is aligned with the NW growth sample. (b) (1) PDMS stamp is pressed into the growth sample, (2) the stage underneath the sample is moved, NWs are captured by the PDMS. (c) captured devices are attached to the surface of PDMS. (d) captured NWs are transferred onto a target disk sample.

The described above NW capture/release process results in a random orientation of the transferred devices on the host sample, see for example image in figure S3(a). The sample was characterized with the automated optical microscopy rig (see reference[2] for further detail on this setup). The characterized devices were located and mapped relatively to the embedded markers. The high-accuracy translation stages of the MTP rig have lateral resolution of ± 25 nm. Therefore, when fully aligned with the markers, it is possible to recover positions of the devices with ~ 1 μm precision. The disk sample is outlined in figure S3(b) with numbers indicating 9 alignment markers on the substrate.

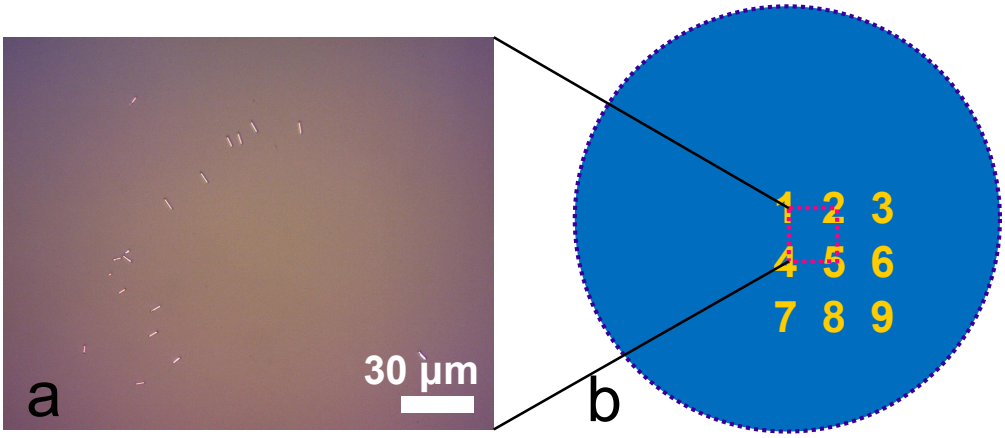

Figure S3: (a) Image of scattered GaAs-InGaAs NW lasers on a quartz disk surface. (b) Schematic diagram of a quartz disk substrate with written markers.

Each identified and characterized NW device was assigned a unique identification number. Figures S4(a-f) show an example of typical characterization information for a NW device. A plot in figure S4(a) shows the device (red dot) location on the disk substrate relatively to the alignment markers (black grids). Processed bright-field images, like that in figure S4(b), were used to estimate the NWs' lengths and their relative orientation to that of the markers. The 'orientation parameter' became crucial when verifying if a specific device was correctly identified, prior to its further integration onto the host disk substrate. Figure S4(c) plots a dark-field micrograph of the lasing emission of the NW when optically pumped laser above its threshold. Figures S4(d-e) depict collected emission spectra of the NW laser at various excitation powers and processed the LILO curve, respectively. The later was used to

calculate the device lasing threshold level. Figure S4(f) shows the measured PL spectrum measurement of the device below its lasing emission threshold. By using the processed data, the NWs were pre-binned and selected for their further transfer printing onto the host substrate.

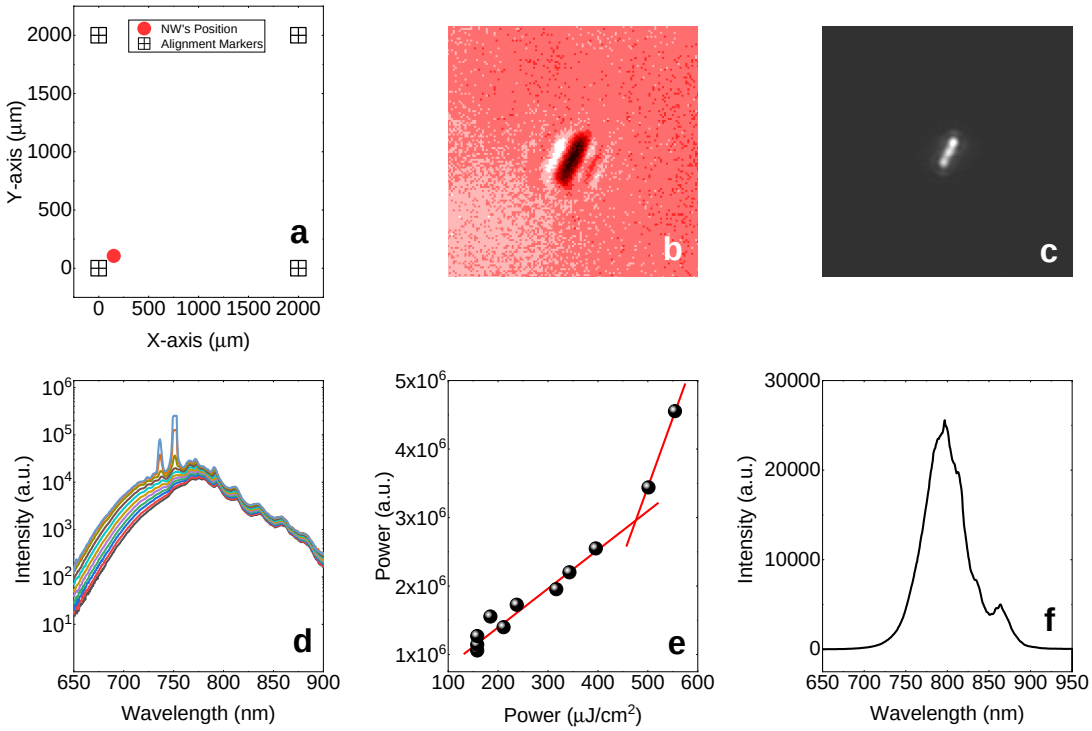

Figure S4: (a) Spatial map showing the location of a NW device. Dark grids indicate alignment markers on the substrate. (b) Image processed bright-field micrograph of the NW laser. (c) Darkfield micrograph of an excited NW laser above its lasing emission. (d) Spectra showing emission wavelength at various excitation energies. (e) A threshold plot showing LILO curve. (f) PL spectra of the NW laser taken at sub-threshold level.

Selected post-processed NW lasers were located and identified on the host sample using the MTP rig. As discussed before, the confocal microscopy module and computer controlled translation stages allowed finding locations of the selected devices in respect to the alignment markers. Moreover, the NW orientation parameter was used to verify the selected device identity. Next, we have used a PDMS μ-stamp (see[3] for description) to transfer individual

devices from the characterization sample onto a target host sample. NWs were transferred one by one printed into arrays with controlled separations. Each array represented different threshold bands, as it can be seen in figure 3(d) of the main manuscript. The process of MTP of individual devices is described in detail[3].

PL Spectrum Analysis

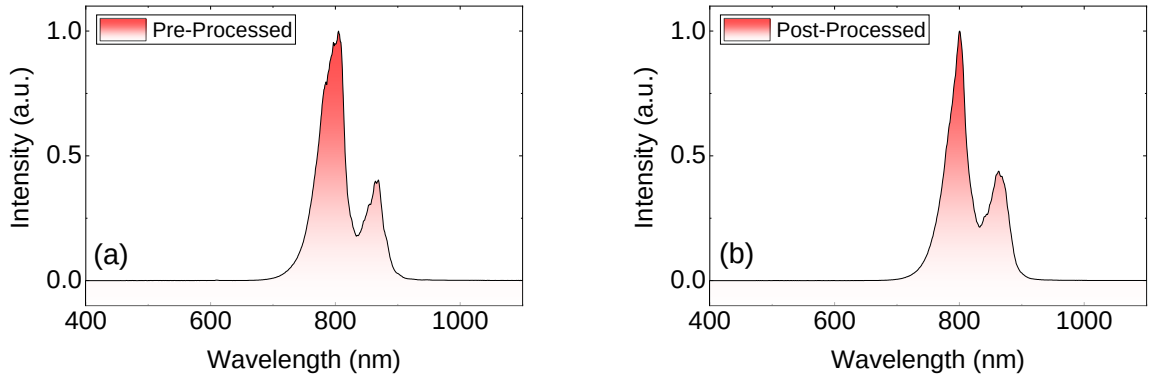

Figure S5: (a) Pre- and (b) post-processed PL spectra of a randomly selected NWs laser.

The NW devices used in this project are multi-quantum well core-shell GaAs-AlGaAs NW lasers. These devices can emit both from its core (E_{core}) and quantum wells (E_{MQW}) at room temperature. Hence, using low power PL measurements (see[2] for a reference) we were able to assess if the NW lasers were damaged during the printing process. This was achieved by evaluating PL emission peaks pre- and post-processing. An example in figures S5(a-b) show two normalized PL emission spectra of a pre- and post-processed device. Analyzed PL plots showed no significant mode shifts or mode suppression between pre- and post-processed devices. Based on that, we conclude that the emission parameters of the MTP lasers were not affected by the described printing processes.

Definition of NW Laser Cases

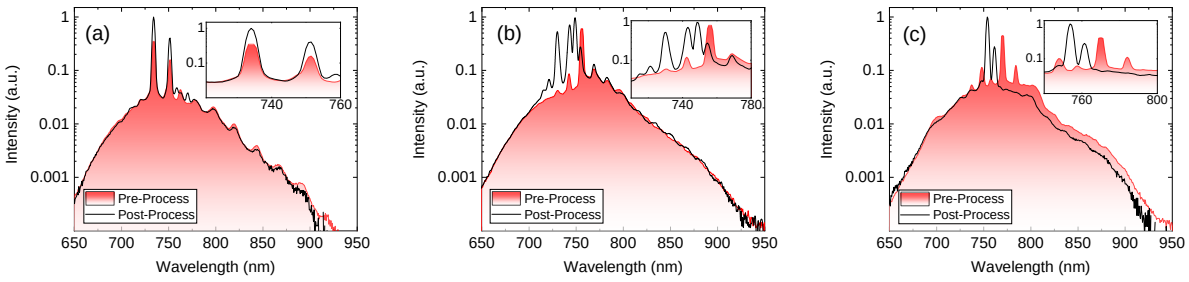

Figure S6: Three representative cases of the printed and un-printed devices which depict state of the spectrum pre- and post-processing: (a) reconstructed, (b) partially reconstructed, (c) non-reconstructed spectrum.

After transferring NW lasers, these were characterized and numerically processed. This allowed the monitoring of their lasing emission parameters. After systematically studying their behavior, three cases were identified showing how the devices performed post-processing. All 98 NW devices that have retained their lasing emission at room temperature were grouped into three individual classes, namely 'A', 'B', and 'C'.

Case 'A' group, shown in figure S6(a), includes NW devices whose FP modes remained the same after the post-processing. Moreover, their peak power corresponding to the wavelength of emission was retained. Effectively, in these devices the lasing spectra was not significantly altered between 1st and 2nd measurement rounds. However, it should be noted that due to the radial asymmetry found in NW lasers[4], their emission radiation is strongly related to their position on a substrate. As a result, in these cases NW lasers are assessed as 'NW-on-substrate' devices, rather than NW behavior independently. Hence, that could partially explain why there are more case 'A' devices in un-printed (45 out of 74) than printed devices (8 out of 24). When re-printing those we change their geometry relative to the substrate orientation, directly affecting device performance.

Figure S6(b) shows case 'B' devices, these contained a group of wires where FP modes overlap with those identified in the pre-processing, however with a changed peak power.

Again, this could be related to the fact that devices/substrate has changed the conditions or the change in the pumping conditions was a significant enough to affect the lasing modes of the devices.

With Case 'C' devices, shown in figure S6(c), the FP modes were not identified with the previously characterized ones, although the PL measurements were comparable with those measured before. It should be noted however, that although it is difficult to explain exactly the nature of these changes, the devices still retained their lasing emission at room temperature.

References

(1) Saxena, D.; Jiang, N.; Yuan, X.; Mokkapati, S.; Guo, Y.; Tan, H. H.; Jagadish, C. Design and Room-Temperature Operation of GaAs/AlGaAs Multiple Quantum Well Nanowire Lasers. *Nano Letters* **2016**, *16*, 5080–5086.

(2) Alanis, J. A.; Saxena, D.; Mokkapati, S.; Jiang, N.; Peng, K.; Tang, X.; Fu, L.; Tan, H. H.; Jagadish, C.; Parkinson, P. Large-Scale Statistics for Threshold Optimization of Optically Pumped Nanowire Lasers. *Nano Letters* **2017**, *17*, 4860–4865.

(3) Guilhabert, B.; Hurtado, A.; Jevtics, D.; Gao, Q.; Tan, H. H.; Jagadish, C.; Dawson, M. D. Transfer Printing of Semiconductor Nanowires with Lasing Emission for Controllable Nanophotonic Device Fabrication. *ACS Nano* **2016**, *10*, 3951–3958.

(4) Davies, C. L.; Parkinson, P.; Jiang, N.; Boland, J. L.; Conesa-Boj, S.; Tan, H. H.; Jagadish, C.; Herz, L. M.; Johnston, M. B. Low ensemble disorder in quantum well tube nanowires. *Nanoscale* **2015**, *7*, 20531–20538.